EVOLUTION OF THE IVGDR AND ITS FINE STRUCTURE FROM DOUBLY-MAGIC ^{40}Ca TO NEUTRON-RICH ^{48}Ca PROBED USING (p,p') SCATTERING*

M.B. Latif, I.T. Usman, J. Carter, E. Sideras-Haddad
L.M. Donaldson, M. Jingo, C.O. Kureba, L. Pellegri

School of Physics, University of the Witwatersrand, Johannesburg 2050, South Africa

R. Neveling, F.D. Smit, F. Nemulodi

Department of Subatomic Physics, iThemba LABS, Somerset West 7129, South Africa

P. von Neumann-Cosel, Y.Yu. Ponomarev

Institute für Kernphysik, Technische Universität Darmstadt, 64289 Darmstadt, Germany

P. Papka, J.A. Swartz

Department of Physics, University of Stellenbosch, Matieland 7062, South Africa

G.R.J. Cooper

School of Geosciences, University of the Witwatersrand
Johannesburg 2050, South Africa

H. Fujita

Research Centre for Nuclear Physics, Osaka University, Ibaraki, Osaka 650-0047, Japan

P. Papakonstantinou

Rare Isotope Science Project, Institute for Basic Science, Daejon 305-811, South Korea

E. Litvinova

Department of Physics, Western Michigan University, Kalanazoo MI 4908-5252, USA

(Received November 21, 2018)

* Presented at the Zakopane Conference on Nuclear Physics "Extremes of the Nuclear Landscape", Zakopane, Poland, August 26–September 2, 2018.

Experiments investigating the fine structure of the Isovector Giant Dipole Resonances (IVGDR) have been carried out on target nuclei ^{40,42,44,48}Ca with 200 MeV proton inelastic scattering reactions using the high-energy resolution capability and the zero-degree set-up at the K600 magnetic spectrometer of the iThemba LABS, Cape Town, South Africa. Quasi-free scattering background contributions in the experimental data have been removed by applying a novel method of Discrete Wavelet Transform (DWT) analysis. Energy scales extracted are compared with the state-of-the-art theoretical calculations within the framework of the Quasiparticle-RPA and Relativistic Quasiparticle Time Blocking Approximation (RQTBA). For ^{40,48}Ca, these calculations consider all major processes (Landau damping, escape width, spreading width) contributing to the damping of the IVGDR.

DOI:10.5506/APhysPolB.50.461

1. Introduction

Giant resonances are a small-amplitude, high-frequency, coherent vibration of nucleons against themselves. As compared to single-particle excitation resonances, giant resonances have a larger strength and width [1]. Giant resonances (GRs) in nuclei are located well above the particle emission threshold and, therefore, decay mainly by particle emission. Significant information about the decay of a giant resonance is contained in the width of the resonance. Recent experimental developments in inelastic hadron scattering with high-energy resolution set-ups have revealed that giant resonances carry fine structure irrespective of the mode. The observed fine structure provides valuable information about factors that contribute to the decay of giant resonances.

A practical way of determining the factors that dominate the decay of the GRs is by establishing a direct comparison between the energy scales extracted from the experimental spectra and those of applicable theoretical calculations. Wavelet analysis allows the extraction of energy scales characterising the fine structure. In the present work, comparison with energy scales derived from microscopic RPA-based models including the coupling to $2p$–$2h$ states is made possible by investigating the role of different mechanisms contributing to the decay widths of the giant resonances. Therefore, the Isovector Giant Dipole Resonance (IVGDR) like any other type of GR results from the collective motion of nucleons. One of the aims in carrying out the present study is to investigate how the fine structure in the IVGDR evolves systematically in calcium isotopes with increased neutron excess. Albeit being the best studied case experimentally and theoretically, many open questions remain, especially in *sd*-shell nuclei.

2. Experiments

The fine structure of the IVGDR has been investigated in the present study using the Separated-Sector Cyclotron (SSC) of the iThemba Laboratory for Accelerator Based Science (iThemba LABS), which delivers high quality proton beams of 200 MeV to the K600 magnetic spectrometer scattering chamber. Self-supporting targets of areal densities $1.5\,\mathrm{mg/cm^2}$, prepared as described in Ref. [2], were made to scatter with a proton beam at an incident energy of $E_p = 200$ MeV and within a spectrometer opening angle of $\theta = \pm 1.91°$. A full description of the experimental setup and the measurement techniques is given in Ref. [3].

The double differential cross-section spectra for the four calcium isotopes are shown in Fig. 1. Pronounced fine structure of the IVGDR can be observed in the energy range of 11–25 MeV in each nucleus, while the compactness in strength is present in the doubly-magic nuclei ^{40,48}Ca. It has been established that the excitation of the $E1$ mode from proton inelastic scattering reaction at and near zero degree is predominantly due to the Coulomb interaction. Also, the (p, p') reaction yields some nuclear background which results from the excitation of other giant resonance modes

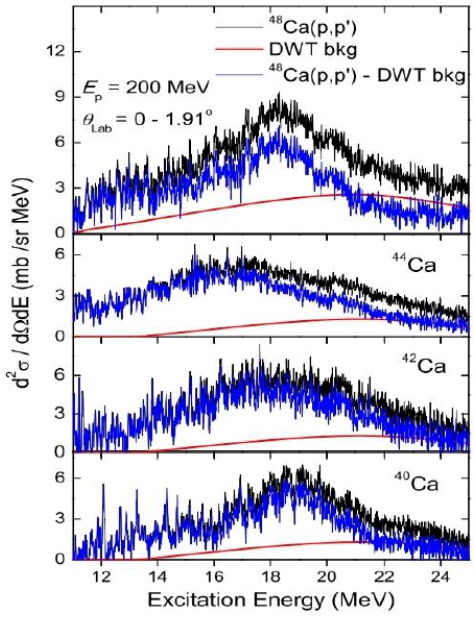

Fig. 1. (Colour on-line) Double differential cross-section spectra showing the region of the IVGDR for ^{40,42,44,48}Ca isotopes (black histogram); the Discrete Wavelet Transform background (DWT bkg) (grey/red line) and the background-subtracted resulting double differential cross section (grey/blue histogram).

and quasi-free scattering. In order to eliminate these contributions, it was assumed that the nuclear background is dominated by quasi-free scattering which can be estimated with the Discrete Wavelet Transform (DWT) spectrum decomposition method. This is in agreement with the calculations in [4] for similar experimental ^{48}Ca data at higher incident energy obtained from the Grand Raiden spectrometer at RCNP.

3. Equivalent photoabsorption cross section

The background subtracted double-differential cross sections computed from the (p, p') spectra (grey/blue histogram of Fig. 1) were converted into equivalent photoabsorption cross sections ($B(E1) \times E_{\mathrm{x}}$) using the following expression [4]:

$$\frac{\mathrm{d}^2\sigma}{\mathrm{d}\Omega \mathrm{d}E} = \frac{1}{E}\frac{\mathrm{d}N_{E1}}{\mathrm{d}\Omega}{\sigma_\gamma}^{E1}, \tag{1}$$

where $\frac{1}{E}\frac{\mathrm{d}N_{E1}}{\mathrm{d}\Omega}$ is the differential virtual photon number per unit energy.

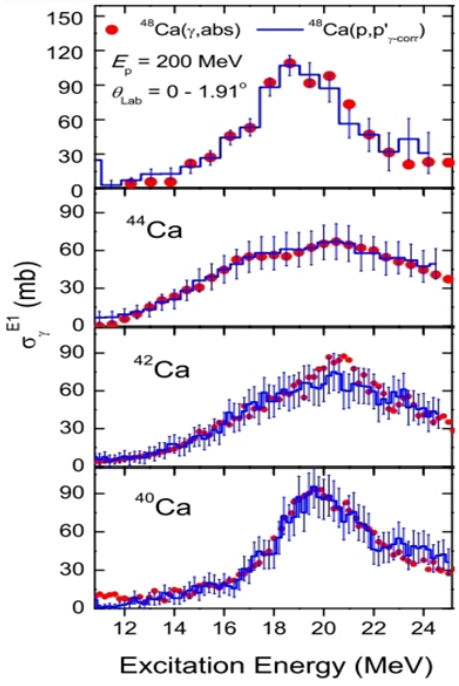

Fig. 2. (Colour on-line) Comparison of normalised experimental photoabsorption cross sections (grey/blue histogram) with the equivalent photoabsorption cross-section data (red circles). Red circle data are presented in 200 keV for ^{40,42}Ca, 500 keV for ^{44}Ca and 796 keV bins for ^{48}Ca.

A comparative plot of the equivalent photoabsorption cross section and the photoabsorption data for ^{40}Ca of Ref. [6], ^{42,44}Ca of Ref. [7] and ^{48}Ca of Ref. [8], respectively, are shown in Fig. 2. From this figure, good agreement between the derived equivalent photoabsorption cross section and the available gamma-absorption data within the limit of experimental error is achieved. It can be clearly observed that the IVGDR exhibits an overall compact shape for ^{40,48}Ca and a broader shape for ^{42,44}Ca. In addition, the resonance shape in ^{44}Ca tends to split into two distinct components whose centroid energies are around 17 MeV and 20 MeV.

4. Theoretical calculations

Investigating the decay of giant resonances provides an avenue for having a better understanding, from a microscopic point of view, of the various mechanisms that contribute to the total width of the resonance. Such an investigation is of paramount importance as giant resonances are strongly damped with a width of only a few MeV. The physical nature of the characteristic energy scales extracted from the fine structure observed in the experimental spectra serves as a basis for interpreting these scales in terms of

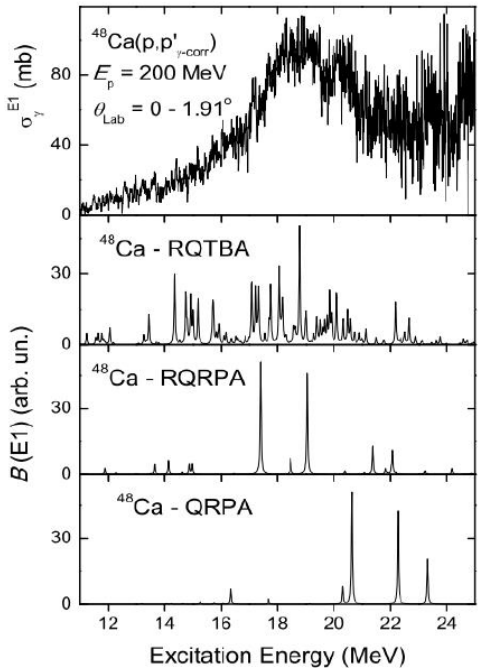

Fig. 3. Experimental (p, p') IVGDR in ^{48}Ca with the theoretical calculations using RQTBA, RQRPA and QRPA.

the various factors that contribute to the total width. Hence, their interpretation can be based on scales extracted from microscopic model calculations of known interaction types in the pairing channels and degrees of freedom.

Understanding, from a theoretical point of view, the connection between the observed fine structure from the experimental spectra and the total width of the resonance requires that the $1p$–$1h$ couples with $2p$–$2h$ through spreading. The mixing of the $1p$–$1h$ and the $2p$–$2h$ configurations by the residual interaction accounts for the spreading width which constitutes the major component of the total width. Comparative plots of the IVGDR strength distribution functions for the experimental data (top panel) and theoretical calculations within the framework of RQTBA, RQRPA and QRPA in ^{48}Ca are shown in Fig. 3 [9, 10]. It can be observed from the strength distribution functions, as illustrated in Fig. 3, that the RQTBA best represents the experimental data in terms of the amount of fine structure exhibited, compared with the other models. Furthermore, this model is observed to exhibit more high-energy strength with increasing neutron number from ^{40}Ca to ^{48}Ca. The RQRPA also exhibits significant amount of fine structure although less than the RQTBA.

5. Wavelet analysis results and discussion

Continuous Wavelet Transform (CWT) analysis [11] was applied to the $(p, p'_{\gamma-\mathrm{corr}})$ data of the experimental calcium isotopes and theoretical calculations, and the obtained characteristic energy scales are compared on a class-to-class basis which is defined by the range of the extracted scale energies. In order to obtain these characteristic scales, a power spectrum of the Wavelet signal (square root of the sum of the absolute values squared of the wavelet coefficients) is applied on the scale axis. The results are shown on the right-hand side of Fig. 4 for ^{48}Ca and Fig. 5 for ^{40}Ca. The various classes of scale energies are defined as follows: Class I: $\Delta E \leq 300$ keV; Class II: 300 keV $\leq \Delta E \leq 1000$ keV; Class III: $\Delta E \geq 1000$ keV.

From the power spectra figures, it can be observed that all the three classes of scales are present in the experimental data. They are also all present in the RQTBA calculations. The RQRPA calculations reproduce reasonably well the Class II and Class III scales of the experimental data. They, however, fail to reproduce the Class I scales in both calcium isotopes.

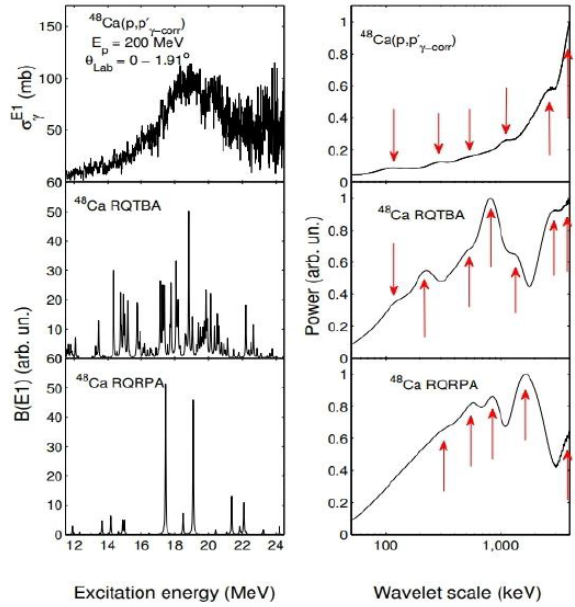

Fig. 4. Power spectra showing energy scales in experimental and theoretical spectra for the ^{48}Ca IVGDR.

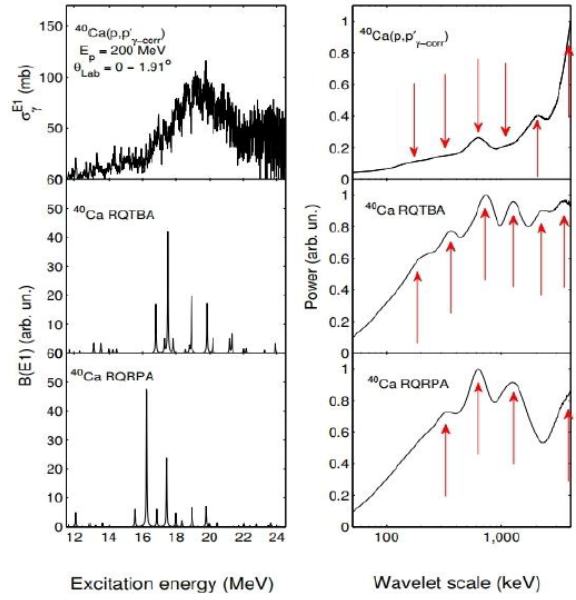

Fig. 5. Power spectra showing energy scales in experimental and theoretical spectra for the ^{40}Ca IVGDR.

6. Conclusions

High energy-resolution inelastic proton scattering measurements at an incident proton energy of $E_p = 200$ MeV and spectrometer angle of $\theta_{\text{scat}} = 0 \pm 1.91^\circ$ were carried out on the even–even stable isotopes of $^{40-48}$Ca. Fine structure is observed in the excitation energy region of the IVGDR. The experimental double differential cross sections were converted into equivalent photoabsorption cross sections by means of virtual photon production rates based on an eikonal approximation. The results show good agreement with the available photoabsorption cross section within limits of experimental error. The role of the various mechanisms that contribute to the decay of the IVGDR was investigated by means of Wavelet analysis of the fine structure in the excitation energy region of the IVGDR. The results show that the Class II and Class III (medium and large) scales present in the experimental spectra are due to the Landau damping with some contribution from the escape width especially for the Class II category.

REFERENCES

[1] M.N. Harakeh, A. van der Woude, *Giant Resonances: Fundamental High-Frequency Modes of Nuclear Excitation*, Oxford University, Oxford 2002.
[2] N.Y. Kheswa *et al.*, *Nucl. Instrum. Methods Phys. Res. A* **613**, 389 (2010).
[3] R. Neveling *et al.*, *Nucl. Instrum. Methods Phys. Res. A* **654**, 29 (2011).
[4] J. Birkhan *et al.*, *Phys. Rev. Lett.* **118**, 252501 (2017).
[5] C.A. Bertulani, A.M. Nathan, *Nucl. Phys. A* **554**, 158 (1993).
[6] J. Ahrens *et al.*, *Nucl. Phys. A* **251**, 479 (1975).
[7] V.A. Erokhova *et al.*, *Bull. Russian Acad. Sci.* **67**, 1636 (2003).
[8] S. Strauch *et al.*, *Phys. Rev. Lett.* **85**, 2913 (2000).
[9] E. Litvinova, P. Ring, V. Tselyaev, *Phys. Rev. C* **78**, 014312 (2008).
[10] E. Litvinova *et al.*, *Phys. Rev. C* **91**, 034332 (2015).
[11] A. Shevchenko *et al.*, *Phys. Rev. C* **77**, 024302 (2008).